Ferromagnetic iron-chromium alloys



1991 J. Phys.: Condens. Matter 3 2089

(http://iopscience.iop.org/0953-8984/3/13/012)

J. Phys.: Condens. Matter 3 (1991) 2089–2099. Printed in the UK

# Ferromagnetic iron–chromium alloys

M E Elzain

Department of Physics, College of Science, PO Box 32486, Sultan Qaboos University, Sultanate of Oman

Received 28 September 1990

**Abstract.** The spin polarized discrete variational method in the local density approximation is used to calculate the electronic structure of 15-atom clusters representing Fe–Cr alloys. The Fe local moment at the central site is found to depend on the orientation (relative to that of Fe) of the Cr moment in the neighbouring shell. For parallel orientation, the Fe moment decreases with increasing number of Cr atoms while it increases slightly in the antiparallel case. The Cr moment dependence on Cr in the NN shell is also determined. These results are incorporated in an approximate relation leading to computation of average moments, and comparison to experimental data is made. It is concluded that there is ferromagnetic coupling between Fe and Cr in the Cr-rich region.

## 1. Introduction

Recent studies have revealed that the local magnetic moment of metal atoms in transition metal alloys depends on their local environment rather than on their average electron properties. The iron–chromium alloys are excellent systems for the study of local environment effects. The elemental iron and chromium have similar BCC lattice structures with very close lattice constants. Moreover, different magnetic interactions exist between the atoms forming the alloy.

Iron–chromium alloys retain the BCC structure over the full concentration range except at intermediate concentrations where a $\sigma$-phase may result under special heat treatment. Although the two species have similar electronegativities the chemical arrangement of the atoms in the alloy is either random or exhibits clustering among similar atoms. The ordered phase is not observed (Hansen 1958). The chemical arrangement of the atoms in the alloy depends very much on the method of preparation and heat treatment (Dubiel *et al* 1984).

As regards the magnetic interactions the general consensus is for antiferromagetic coupling between Fe and Cr atoms (Anisimov *et al* 1988). However, ferromagnetic interactions between Fe–Cr and Cr–Cr atoms and antiferromagnetic interaction between Fe–Fe atoms may arise, at least in frustrated configurations. The presence of such diverse interactions lead to a complex magnetic structure. Indeed, the magnetic phase diagram of Fe–Cr alloys consists of a ferromagnetic (FM) region for Fe concentrations in excess of 19 at.%, followed by spin glass (SG) phase in between 19 and 16 at.% Fe and then an antiferromagnetic (AFM) phase down to about 2% (Burke *et al* 1983). Below this spin density waves dominate the magnetic structre. The boundary regions between FM and SG, and AFM and SG are blurred by re-entrant spin glass phases (Dubiel *et al* 1984, 1985, Shull and Beck 1974).

0953-8984/91/132089+11$03.50  

In the FM region the measured average local moment per atom (Aldred 1976, Besnus and Meyer 1970) and the magnetic hyperfine field at the Fe site (Kuwano and Ono 1977) decrease linearly with decreasing Fe concentration. However, it does not vanish at the critical concentration. The persistence of the average local moment below 19 at.% Fe was regarded as an overestimation due to the high fields used in the magnetization measurements (Burke *et al* 1983). The Fe local moment, which increases initially, decreases slightly on further Cr addition while the oppositely oriented Cr moment goes rapidly to zero (Aldred *et al* 1976). Near The FM–SG boundary the experimental results are conflicting and the situation is far from clear. While finite Fe local moments were reported in this region (Aldred 1976, Besnus and Meyer 1970) others detected spin glass state (Dubiel *et al* 1984).In general it appears there is disagreement between Mössbauer measurement and the other measurements. Dubiel *et al* (1984) suggested that the existence of a split Mössbauer spectrum does not necessarily mean that the whole system is magnetically ordered.

On the theoretical side, HF-CPA was used to calculate the zero-temperature electronic and magnetic structures (Hasegawa and Kanamori 1972, Jo 1983). The average local moment was found to decrease to zero with Cr addition. Similar results were obtained by Kakehashi (1987) at finite temperatures using the local environment effect method. The Fe and Cr local moments were found to depend on the number of Cr NN as well as on concentration and both were found to vanish at the critcal concentration. This is in contrast with the Maksymowicz (1982) calculation. Maksymowicz, using the continued fraction method, obtained a finite Fe moment over the full concentration range. In addition Kakehashi, using a phenomenological relation between magnetic hyperfine field and the average local moment, obtained magnetic hyperfine field distributions that are close to experimental results. The calculation of those distributions rested on the assumption that the Fe local moment vanishes which may not be the case.

In the AFM phase the measured sublattice magnetization and the Néel temperature, which are proportional, were found to decrease with increasing Fe concentration (Burke and Rainford 1978). Mössbauer measurement gave a small local moment of a maximum of 0.5 Bohr magnetons (Herbert *et al* 1972). Magnetization (Ishikawa *et al* 1967), magnetic susceptibility (Ishikawa *et al* 1965) and polarized neutron scattering (Moze *et al* 1988) measurements gave a large Fe local moment which is of the order of two Bohr magnetons. These contradictory results were attributed to the presence of superparamagnetic Fe pairs which are weakly coupled to the Cr AFM matrix (Friedel and Hedman 1978). However, Mössbauer measurement at temperatures on the mK scale, where the thermal fluctuation of the superparamagnetic Fe pairs is expected to be less vigorous, did not show any additional line broadening when compared to the spectrum at 4.2 K (Shinjo *et al* 1974). This makes the existence of these weakly coupled superparamagnetic pairs unlikely.

On the basis of Mössbauer measurements Shiga and Nakamura (1980) proposed a model for the magnetic structure of Fe–Cr alloys. It was proposed that Cr atoms retain a zero moment and the Fe atoms have magnetic and non-magnetic species. The non-magnetic Fe atoms, which are isolated atoms, have a zero moment and hyperfine field. The magnetic Fe atoms resulting from an environment rich in Fe, possess a constant local moment. However, some of these latter atoms couple antiferromagnetically, reducing the average moment. Shiga and Nakamura found that the magnetic hyperfine field associated with the non-magnetic component persists to concentrations extending up to 30 at.% Fe, where the alloy is FM with a relatively high Curie temperature.

In this paper we use the first principle discrete variational method in the local density approximation, section 2, to calculate the local magnetic moment at Fe and Cr sites in different cluster configurations. The results are presented and discussed in section 3. In subsection 3.1 we attribute the conflict between Mössbauer and magnetization measurement to the difference in terms contributing to the magnetic hyperfine field and those contributing to the average magnetic moment. In subsection 3.2 we develop an approximate relation giving each of the local quantites for every configuration. Comparison to experimental results is made in subsection 3.3. In this paper we limit ourself to the FM region. In the last section we give a summary of our results.

## 2. Calculational model

15-atom clusters were taken as representing Fe and Cr atoms in BCC Fe–Cr alloys. Fe-centred and Cr-centred clusters are denoted by Fe$[P, N, Q, M]$ and Cr$[P, N, Q, M]$, respectively. $P$ and $Q$ are the numbers of Fe atoms in the nearest neighbour (NN) and next nearest neighbour (NNN) shells respectively, while $N$ and $M$ stand for the numbers of Cr atoms in the respective shells which have their moment oriented parallel to that of Fe. The discrete variational method (Averil and Ellis (1973) and references therein) in the spin polarized local density approximation is used to calculate the eigenstates of the Kohn–Sham equation with the von Barth–Hedin exchange–correlation potential.

The self-consistent calculation of the valence eigenstates was performed using as variational basis a linear combination of atomic orbitals 3d, 4s and 4p, while the core states were kept frozen. The matrix elements of the Hamiltonian and overlap matrices were obtained by numerical integration. The pseudorandom diophantine integration method is augmented as desired by a special integration scheme in spherical volume about particular atoms. Average properties such as atomic configuration, energy levels and magnetic moments converge rapidly with the diophantine sample, with 300–400 points per atom being sufficient to determine such properties to better than experimental precision. Properties such as contact spin and charge densities which depend sensitively upon wave function in the atomic core region require a more careful solution of the Kohn–Sham equation in the region of the probe nucleus. In this region the diophantine points are replaced by a dense regular (angular × Gaussian quadrature) mesh.

Different magnetic configurations are obtained through selection of relevant initial magnetic moment inputs. However, in some cases the solution does not converge to the desired magnetic configuration but rather to another configuration dictated by the intrinsic exchange–correlation interaction. For example, it was not possible to get a solution for the cluster Fe$[0, 8, 0, 6]$, where all Cr atoms have upward moments. The cluster approach offers a flexiblity in studying the effect of the surrounding atoms on the central atom upto one at a time. It is not limitted by any symmetry requirement such as a unit cell. But, it introduces surface effects which might be serious in the case of non-local properties. For local properties it gives reasonable values.

The contributions to the magnetic hyperfine $B_{\mathrm{hf}}$ at the Fe site come mainly from the Fermi contact term. This is the difference between spin-up and spin-down densities at the origin. Each spin density can be split into core and valence contributions. The core contribution scales linearly with the local 3d moment (Elzain *et al* 1986, Blugel *et al* 1987). Since in our calculation the core states are frozen we estimate the core contribution to $B_{\mathrm{hf}}$ from the local 3d moment. Hence, we employ the phenomenological

relation:

$$B_{\rm hf} = -A\mu_{\rm d} + C(\varrho_{+}(0) - \varrho_{-}(0)) \tag{1}$$

where the first term represents the core contribution and the second the valence part. $\mu_{\rm d}$ is the local 3d Fe moment and a value of 10 T per Bohr magneton is taken for the constant $A$ (Elzain *et al* 1986, Blugel *et al* 1987). $\varrho_{\sigma}$ is the valence density at the origin for up and down spins. The constant $C$ equals 52.4 when $B_{\rm hf}$ is in teslas and the spin density in atomic units. A similar approach, in spirit, for the estimation of $B_{\rm hf}$ was used by Campell *et al* (1977) and Dubiel *et al* (1978), where the importance of the valence contribution to the hyperfine field was stressed. The difference between equation (1) and the latter approach is that we calculate the valence contribution directly without resorting to average moments. Further, we found that the core contribution is proportional to the 3d local moment rather than to the total moment as used by Campell *et al* (1977) and Dubiel *et al* (1978).

## 3. Results and discussions

### *3.1. Local properties*

Table 1 shows the total magnetic moment $\mu$, the valence contact spin density $\Delta\varrho$ and $B_{\rm hf}$ at the central Fe site in Fe15 clusters calculated using $O_h$, $D_{4h}$ and $C_{2v}$ point groups. Mulliken population analysis is used to calculate $\mu$ while equation (1) is employed for the calculation of $B_{\rm hf}$. The purpose of this calculation is twofold. Firstly, since $\mu$, $\Delta\varrho$ and $B_{\rm hf}$ for $\alpha$-Fe are well known (Lindgren (1988) and references therein) their close comparison to Fe15 results gives confidence in the correspoding results for Fe–Cr clusters. Secondly, we employed the $C_{2v}$ point group in most of our calculation and the close comparison of the results for Fe15 clusters among themselves indicates that symmetry has a marginal effect.

For Fe–Cr alloys there are more than a thousand different possible configurations with differing atomic types and Cr orientation in NN and NNN shells. We did calculations for a number of these cluster configurations (33 in all) for the purpose of testing the variation of local properties versus chemical and magnetic changes of the local environment.

Results for extreme Fe-centred clusters are shown in table 2. These clusters are extreme in the sense that the numbers $P$, $Q$, $N$ and $M$ take either their maximum or minimum values. The last two clusters represent Fe in Cr. The Cr atoms in the NN shell have antiparallel and parallel orientations for the first and the second of these latter clusters respectively. We note that for fixed $Q$ and $M$ there is a major decrease in Fe moment when Cr reverses its orientation from antiparallel to parallel. The opposite occurs, however, at a lower rate, when the Cr moment in NNN shells changes direction. We found this to be true in general for all computed Fe moments. The Fe moment increases slightly when Fe atoms in the NN shell are replaced by Cr atoms with opposite moment as comparison of the Fe moment in table 1 with that of Fe[0, 0, 6, 0] would show.

The striking features exhibited by the contact spin density and hyperfine field are firstly the large positive values obtained for Fe[0, 0, 6, 0]. This cluster would represent Fe–Cr alloys in a perfect CsCl structure with all Cr moments being antiparallel to that of Fe. Observation of positive $B_{\rm hf}$ may signal the existence of a Fe–Cr chemically

ordered phase. The $B_{hf}$ measured thus far are negative except in one measurement (Blum and Grodzins 1964) which was later rectified to give a negative field (Herbert *et al* 1972). Secondly, the hyperfine field at Fe sites in Fe[0,0,0,6] and Fe[0,8,0,0] is vanishingly small although the local moment is large. This is a point to be noted since then the absence of a Mössbauer split spectrum would not necessarily mean the absence of magnetic order.

**Table 1.** The local magnetic moment $\mu$ in Bohr magnetons, the contact spin density $\Delta\varrho$ in atomic units and the magnetic hyperfine field $B_{hf}$ in teslas at an Fe site in Fe15 clusters for $O_h$, $D_{4h}$ and $C_{2v}$ symmetries.

| | $O_h$ | $D_{4h}$ | $C_{2v}$ |
|---|---|---|---|
| $\mu$ | 2.12 | 2.14 | 2.14 |
| $\Delta\varrho$ | −0.23 | −0.21 | −0.19 |
| $B_{hf}$ | −35.3 | −34.5 | −33.4 |

**Table 2.** The local magnetic moment $\mu$ in Bohr magnetons, the contact spin density $\Delta\varrho$ in atomic units and the magnetic hyperfine field $B_{hf}$ in teslas at an Fe site in representative Fe-centred clusters.

| | $\mu$ | $\Delta\varrho$ | $B_{hf}$ |
|---|---|---|---|
| Fe[0,0,6,0] | 2.31 | 0.92 | 27.8 |
| Fe[0,8,6,0] | 1.24 | 0.08 | −9.4 |
| Fe[8,0,0,0] | 1.88 | −0.02 | −19.3 |
| Fe[8,0,0,6] | 2.55 | −0.09 | −31.8 |
| Fe[0,0,0,6] | 2.46 | 0.44 | −0.5 |
| Fe[0,8,0,0] | 1.07 | 0.24 | 1.0 |

**Table 3.** The local magnetic moment $\mu$ in Bohr magnetons at Cr site in representative Cr-centred clusters.

| | Cr[0,0,0,6] | Cr[0,0,6,0] | Cr[0,8,6,0] | Cr[8,0,0,0] | Cr[8,0,0,6] | Cr[8,0,6,0] |
|---|---|---|---|---|---|---|
| $\mu$ | 2.02 | 2.30 | −1.19 | −0.53 | −0.78 | −0.98 |

Table 3 shows the Cr local moment for some extreme Cr-centred clusters. Local moments were calculated for 19 different clusters. The first cluster in table 3 represents a Cr atom in the positively oriented sublattice of the antiferromagnetically ordered Cr. The Cr atoms on the other sublattice have the exactly opposite moment. These moments are larger than those obtained using the LMTO Green function method (Anisimov *et al* 1988). This could be regarded as a cluster size effect on Cr metal where the actual magnetic structure exhibits a true spin density modulation instead of a local magnetic character. However, our interest is not in pure Cr but rather in its Fe alloys and these alloys are AFM in the Cr-rich region. Furthermore, we note that the magnitude of the Cr moment decreases with increasing Fe content, reaching a value of about −1 Bohr magnetons for Cr moment in pure Fe. This value agrees with the neutron scattering results (Aldred *et al* 1976); however, its magnitude is small compared with the LMTO Green function calculation (Antropov *et al* 1988).

*3.2. Configuration dependence of local properties*

To be able to compare these results to the experimental data we need to take averages over all possible configurations. It is a formidable task to perform the calculation for each and every individual configuration. We have seen in subsection 3.1 above that the the local moment and contact spin density depend on $P$, $Q$, $N$ and $M$. Calculation of the local properties of Fe$[0,N,6,0]$ for $N = 0$, 2, 4 and 6 led to a linear dependence of these quantities on $N$. Figure 1 shows the change in Fe local moment versus $N$ for the Fe$[0,N,6,0]$ clusters. The straight line is the result of equation (2) below. Variations against $N$ for other clusters reflected the same pattern. Also similar trends were observed with changes in $M$. On this basis we assumed a linear dependence on $N$ and $M$ and their complimentary values $8-N$ and $6-M$ which are the numbers of Cr atoms with antiparallel orientation. We denote $N$, $8-N$, $M$ and $6-M$ collectively by $X_{j\sigma}$, where $j = 1$ and 2 for NN and NNN shells respectively and $\sigma$ defines the Cr orientation. A local property $Y$ is then expressed as

$$Y = Y_0 + \sum m_{j\sigma} X_{j\sigma}. \tag{2}$$

$Y_0$ is the value of the local quantity in iron, i.e. when all the atoms surrounding the central one are Fe atoms. The coefficients $m_{j\sigma}$ depend on the total number of Cr atoms in each subshell. We found that this dependence is also fairly linear. Hence we write

$$m_{j\sigma} = \alpha_{j\sigma}(1 - Z_j/Z_j^0). \tag{3}$$

$Z_j$ is the number of Fe atoms in NN or NNN shells and $Z_1^0 = 8$, $Z_2^0 = 6$. The coefficients $\alpha_{j\sigma}$ are now constants and their values depend only on the associated property.

The coefficients $\alpha_{j\sigma}$ could be calculated by fitting equation (2) to all the numerically computed values for each property. However, the values determined by equating equation (2) to the results of the clusters shown in table 2 and 3 were found to be quite satisfactory. The values calculated for other configurations using equation (2) with the aforementioned coefficients were found to be in reasonable agreement with the corresponding first principle computed values.

The coefficients corresponding to Fe local moments are $Y_0 = 2.14$, $\alpha_{1+} = -0.11$, $\alpha_{1-} = 0.02$, $\alpha_{2+} = 0.07$, $\alpha_{2-} = -0.04$ and those corresponding to Cr local moments are $Y_0 = -0.98$, $\alpha_{1+} = -0.2$ to $-0.1$ (weakly dependent on $Q$-values), $\alpha_{1-} = 0.38$, $\alpha_{2+} = 0.03$ and $\alpha_{2-} = 0.08$. Except for the Fe moment coefficient, $\alpha_{1-}$, we note that the coefficients for variations against NNN atoms are a factor of 2 to 3, or more, smaller than the corresponding NN coefficients. Hence if such a relation is to be extended to third and further shells the influence of these further shells on the local moments is expected to be smaller. The small Fe coefficient $\alpha_{1-}$ reinforces the previously stated observation that Fe moment changes slightly when an Fe atom in a NN shell is replaced by an antiparallel-oriented Cr atom.

Figure 2 shows the variation of Fe and Cr local moments versus the number of Fe atoms $P$. The dependence is non-linear since equation (2) is in fact non-linear in $Z_j$. This agrees, in trends, with the experimentally reported variations (Shiga and Nakamura 1980). The two branches of local moments of each atom correspond to configurations where all Cr moments in the NN shell are either parallel or antiparallel to the Fe moment. The Fe moment in all clusters is taken in the upward direction, i.e. all Fe–Fe atoms couple ferromagnetically. Antiferromagnetic coupling between Fe

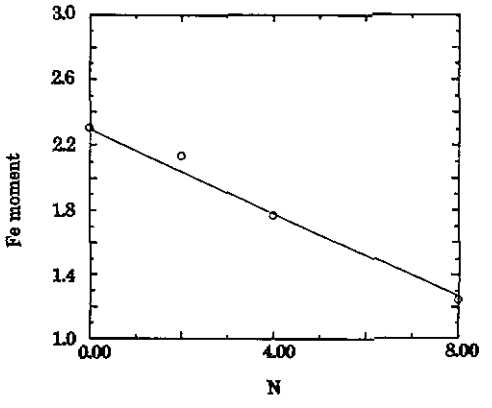


**Figure 1.** The Fe local moment in Bohr magnetons versus the number of parallel oriented Cr atoms in the NN shell of the central Fe atom in Fe$[0, N, 6, 0]$ clusters. The open circles are the moments calculated from first principles. The straight line represents values calculated using equation (2).

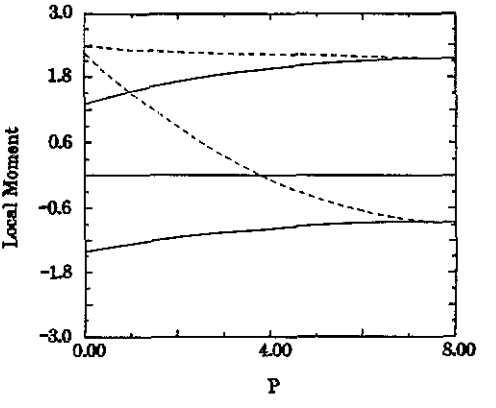


**Figure 2.** The local Fe and Cr moments, in Bohr magnetons, calculated according to equation (2) versus the number of Fe atoms in the NN shell. The upper curves represent the Fe moment while the lower curves represent that of Cr. Full curves, all NN Cr moments are pointing upward; broken curves, all NN Cr moments are pointing downward.

atoms has not been considered. Such a coupling may arise in the FM Cr-rich region and in the SG and the AFM phases.

For the hyperfine field calculation we obtained the coefficients for the 3d Fe moment and the spin density at the Fe site in the same fashion. Then equation (1) is used to calculate $B_{\mathrm{hf}}$ in different configurations.

### *3.3. Average properties*

The calculations of average quantities over the cluster configuration are performed assuming a binomial distribution of Fe atoms in the Cr matrix. An atomic short range order parameter (ASROP), $b$, is included in the site occupation probability $x = c \pm bc(1-c)$, where $c$ is the Fe concentration. We distinguish three sites:

(i) the Fe site where the moment is always positive;
(ii) Cr sites with NN Cr atoms having positive moment; and
(iii) Cr sites with NN Cr atoms having negative moment.

The Cr sites correspond to the perfect AFM sublattices in Cr-rich regions. The local moments at these two sites converge to the same value in the Fe-rich region, figure 2. We assume that these two sites are available in equal proportions. Their contribution to the average moment is governed by the probability of orientation, $p$, of the Cr moment in the NN shell.

Using the binomial distribution the average local moments $\langle \mu^{\mathrm{Fe}}(c,b,p) \rangle$ and $\langle \mu_{\sigma}^{\mathrm{Cr}}(c,b,p) \rangle$ at Fe and Cr sites, respectively, are calculated (Elzain and Ellis 1987). The average total moment $\langle \mu(c,b,p) \rangle$ is then obtained by adding the three moments in the right proportions

$$\langle \mu(c,b,p) \rangle = c\langle \mu^{\mathrm{Fe}}(c,b,p) \rangle + (1-c)[\langle \mu_{+}^{\mathrm{Cr}}(c,b,p) \rangle + \langle \mu_{-}^{\mathrm{Cr}}(c,b,1-p) \rangle]/2. \tag{4}$$

For comparison with experimental results we scaled the calculated average moments by the Fe15 cluster moment and the experimental moments by the corresponding experimental pure Fe moment. The comparison then reflects the trends rather than the actual magnitudes. Such scaled comparison should incur no lack of credibility on the cluster results since, in any case, clusters cannot reproduce the exact properties of macroscopic systems. The relative changes in the averaged properties and not their magnitudes are the quantities which would help in understanding the mechanisms bringing those changes.

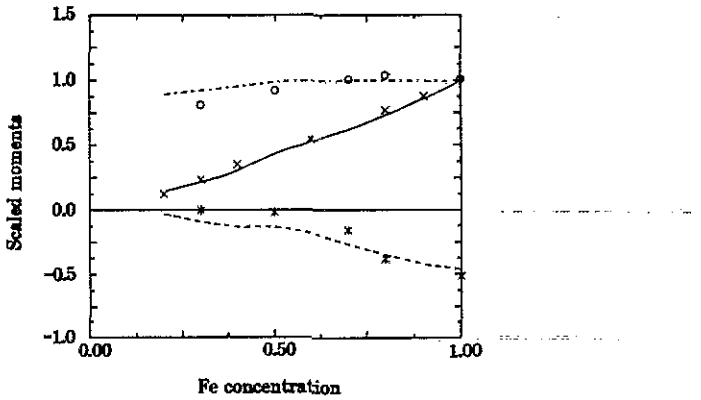


**Figure 3.** The scaled average moments against Fe concentration. The full line represents the calculated average moment according to equation (3) and the crosses are the scaled experimental results of Aldred (1976) and Besnus and Meyer (1970). These experimental data coincide. The upper broken curve and the open circles are the respectively, calculated and experimental (Aldred *et al* 1976) scaled average Fe local moments. The lower broken curve and the stars are the scaled calculated and experimental (Aldred *et al* 1976) average local moments at Cr site, respectively.

The calculated average moment for a weakly clustered chemical arrangement and Cr moment orientation probability $p \sim 0.5$, together with the experimental data of Aldred *et al* (1976) and Besnus and Meyer (1970), are shown in figure 3. Clustering occurs in the Fe-rich region while in the Cr-rich region complete disorder prevails. The average moments are seen to be in fair agreement with the experimental data. However, this is at the expense of allowing FM coupling between Fe and Cr. Inclusion of this interaction affects the moments in the Cr-rich region only. The moments in the Fe-rich region were found to be insensitive to changes in $p$. This is a physically sound observation since in the latter region all Cr moments are in the antiparallel orientation, i.e. $p \sim 1$. The average calculated moment does not vanish at the critical concentration. This is, in our view, because near the critical region AFM couplings between Fe atoms may arise and persist right through the spin glass and AFM regions. In this case a further Fe site is required in addition to the aforementioned sites. Such a site is currently under consideration.

The hyperfine field distributions have been calculated using a Lorentzian function of width about 2 T which is summed over all Fe configurations. We found the distributions in the Fe-rich region to be centred around large and negative hyperfine fields in agreement with experiments. This is a region of no basic differences. Towards the

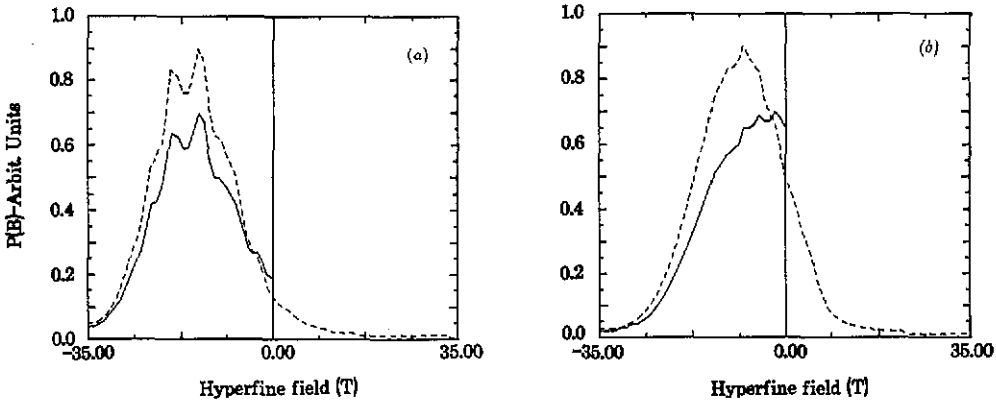


**Figure 4.** The hyperfine field distribution at Fe concentration c = 0.20 for the more dominant case of (*a*) AFM and (*b*) FM couplings between Fe and Cr. The broken curve represents the distribution over the full range of the hyperfine fields and the full curve, that for the case when all the fields are considered as negative. The two curves are shifted to avoid overlapping.

frontiers of the Cr-rich region conflicts arise. For example Curie temperatures determined through Mössbauer measurement are usually lower than those obtained through magnetization measurements (Dubiel *et al* 1984, Loegel *et al* 1975). In figure 4 we show the hyperfine field distribution for $c = 0.2$. In figure 4(*a*) the distributions over the full range of $B_{\rm hf}$ (positive and negative) and over the negative range only are shown for the case where AFM interactions between Fe and Cr are more dominant. Figure 4(*b*) shows the FM case. The distributions limited to the negative part of the hyperfine field axis are obtained by counting the contribution of the positive field as if it is due to a corresponding negative field. Then if the Fe–Cr interaction changes with temperature the magnetization and Mössbauer measurment will be in accord. Ferromagnetic interactions will dominate at high temperatures and AFM interactions at low temperatures. At further lowered temperatures Fe–Cr systems undergo a transition to a reentrant spin glass phase (Dubeil *et al* 1985, Kunitomi *et al* 1986), indicating the presence of more antiferrmagnetic couplings. Nieuwenhuys *et al* (1979) have emphasized the role of the exchange interaction and its variation with temperature as a determining factor for the magnetic state of Fe alloys.

Although it is not within the scope of this work we note that in the AFM phase at dilute Fe concentrations the local Fe moment remains finite and large while the magnetic hyperfine field is vanishingly small. This explains the differences in values reported for the Fe local moment through Mössbauer, magnitization and susceptibility measurements without the need for invoking Fe pair superparamagnetism.

## 4. Conclusion

We have calculated the local Fe moment, its magnetic hyperfine field and Cr local moment in different magnetic clusters representing FM Fe–Cr alloys using the discrete variational method. The effects of chemical and magnetic changes in the local environment of the central atom were studied. In particular it was found that:

(i) The Fe local moment increases slightly when a Cr atom replaces an Fe atom in the NN shell provided that the Fe–Cr coupling is antiferromagnetic. However, the Fe moment is reduced when the coupling is ferromagnetic.

(ii) The magnetic hyperfine field at the Fe site is reduced by the presence of Cr atoms of any orientation and it becomes zero or even positive while a large local Fe moment is retained.

(iii) The Cr local moment in an Fe-rich environment is negative and it changes sign or becomes more negative with increasing Cr content.

These findings were elaborated reaching an approximate relation between the local quantities and their local environment variables. This relation was used to calculate the average quantities for the sake of making comparison to experiments. It was found that the experimental average moments could be well represented when a FM coupling between Fe and Cr is allowed for in the Cr-rich region. We conjectured that a temperature dependent coupling between Fe and Cr would resolve the conflict between the Curie temperatures determined from the Mössbauer and magnetization measurements. We also pointed out that a large Fe local moment is reconcilable with a small hyperfine field in the AFM phase, making the Mössbauer and magnetic measurements compatible.

## Acknowledgments

The author would like to thank Professor Abdus Salam, the International Atomic Energy Agency, and UNESCO for hospitality at the ICTP (International Centre for Theoretical Physics), Trieste, Italy.

## References

Aldred A T 1976 *Phys. Rev.* B **14** 219
Aldred A T, Rainford B D, Kouvel J S and Hicks T J 1976 *Phys. Rev.* B **14** 228
Anisimov V I, Antropov V P, Liechtenstein A I, Gubanov V A and Postnikov A V 1988 *Phys. Rev.* B **37** 5598
Antropov V P, Anisimov V I, Liechlenstein A I and Postnikov A V 1988 *Phys. Rev.* B **37** 5603
Averil E W and Ellis D E 1973 *J. Chem. Phys.* **59** 6412
Besnus M J and Meyer A J 1970 *Phys. Rev.* B **2** 2999
Blugel S, Akai H, Zeller R and Dederchs P H 1987 *Phys. Rev.* B **35** 327
Blum N A and Grodzins I 1964 *Phys. Rev.* **136** A33
Burke S K, Cywinski R, Davis J R and Rainford B D 1983 *J. Phys. F: Met. Phys.* **13** 451
Burke S K and Rainford B D 1978 *J. Phys. F: Met. Phys.* **8** 1239
Campell C C M, Birchall T and Suits J C 1977 *J. Phys. F: Met. Phys.* **7** 727
Dubiel S M, Campell C C M and Obuszko Z 1978 *Solid State Commun.* **26** 593
Dubiel S M, Saucer Ch and Zinn W 1984 *Phys. Rev.* B **30** 6285
—— 1985 *Phys. Rev.* B **31** 1643
Elzain M E and Ellis D E 1987 *J. Magn. Magn. Mater.* **67** 128
Elzain M E, Ellis D E and Guenzburger D 1986 *Phys. Rev.* B **34** 1430
Friedel J and Hedman L E 1978 *J. Physique* **39** 1225
Hansen P M 1958 *Constitution of Binary Alloys* (New York: McGraw-Hill) p 525
Hasegawa H and Kanomori J 1972 *J. Phys. Soc. Japan* **33** 1607
Herbert I R, Clark P F and Wilson G V H 1972 *J. Phys. Chem. Solids* **33** 979
Ishikawa Y, Hoshino S and Endoh Y 1967 *J. Phys. Soc. Japan* **22** 1221
Ishikawa Y, Tournier R and Philippi J 1965 *J. Phys. Chem. Solids* **26** 1727
Jo T 1983 *J. Magn. Magn. Mater.* **31–34** 51

Kakehashi Y 1987 *Phys. Rev.* B **35** 4973
Kunitomi N, Nakai Y, Tsuge S, Yamamoto N and Fujita K 1986 *Hyperfine Interact.* **28** 515
Kuwano H and Ono K 1977 *J. Phys. Soc. Japan* **42** 72
Lindgren B 1988 *J. Phys. F: Met. Phys.* **18** 1563
Loegel B, Friedt J M and Poinsot R 1975 *J. Phys. F: Met. Phys.* **5** 154
Maksymowicz A Z 1982 *J. Phys. F: Met. Phys.* **12** 537
Moze O, Mitchell P W, Burkes S K, Davis J R and Booth J G 1988 *J. Phys. F: Met. Phys.* **18** 527
Nieuwenhuys J, Verbeek B H and Mydosh J A 1979 *J. Appl. Phys.* **50** 1685
Shiga M and Nakamura Y 1980 *J. Phys. Soc. Japan* **49** 528
Shinjo T, Okada K, Takada T and Ishikawa Y 1974 *J. Phys. Soc. Japan* **37** 877
Shull R D and Beck P A 1974 *AIP Conf. Proc.* **24** 95